Diffraction Shader

Michael Single

15. Januar 2014

Inhaltsverzeichnis

1 Introduction

1.1 Motivation

In Nature, coloring mostly comes from the inherent colors of materials but sometimes colorization has a pure physical origin such as the effect diffraction or interference of light. Both phenomenon are causing the so called structural coloration, which is the production of color through the interaction of visible light with micrioscopically structured surfaces. Color production is die to wave interference with quasiperiodic structures whose periodicity leads to interaction with visible light. Therefore we perceive color when the different wavelengths composing white light are selectively interfered with by matter (absorbed, reflected, refracted, scattered, or diffracted) on their way to our eyes, or when a non-white distribution of light has been emitted. In animals, such as feathers of birds and the scales of butterflies, interference is created by a range of photonic mechanisms, including diffraction grating, selective mirrors, photonic crystals. The connection beween microscopic structures and coloration has been observed by Robert Hooke in the early seventeenth centrury. The discovery of the wave nature of light led to the conclusion that the cause for the coloration lies in wave interference.

In the field of computer graphics, many researchers have been attempted rendering of structural colors by formulating a the bidirectional reflectance distribution function (BRDF) for this purpose. But most of the techniques so far, however, are either too slow for interactive rendering or rely on simplifying assumption, like modeling light as rays, to achieve real-time performance, which are not able capturing the essence of diffraction at all.

1.2 Goals

The purpose of this thesis is to simulate realistically by rendering structural colors caused by the effect of diffraction on different biological structures in realtime. We focus on structural colors generated by diffraction gratings, in particular our approach applies to surfaces with quasiperiodic structures at the nanometer scale that can be represented as heighfields. such structures are found on the sehds of snkaes, wings of butterflies or the bodies of various insects. we restrict ourself and focus on different snake skins sheds which are acquired nanoscaled heightfields using atomic force microscopy.

In oder to achieve our rendering purpose we will rely J. Stam's formula-

tion of a BRDF which basically describes the effect of diffraction on a given surface assuming one knows the hightfield of this surface and will further extend this. Appart from Stam's approach, which models the heightfield as a probabilistic superposition of bumps and proceeds to derive an analytical expression for the BRDF, our BRDF representation takes the heightfield from explicit measurement. I.E. in our case, those heightfields are small patches of the microstructured surfaces (in nano-scale) taken by AFM of snake skin patches provided by our collaborators in Geneva.. So this approach is closer to real truth, since we use measured surfaces instead of statistical surface profile.

Therefore, this work can be considered as an extension of J. Stam's derivations for the case one is provided by a explicit height field on a quasiperiodic structure.

Real time performance is achieved with a representation of the formula as a power series over a variable related to the viewing and lighting directions. Values closely related to the coefficients in that power series are precomputed.

The contribution is that this approach is more broadly applicable than the previous work. Although the previously published formula theoretically has this much flexibility already, there is a novel contribution in demonstrating how such generality can be leveraged in practical implementation

1.3   Previous work

stam, hooke, see our paper, see stams paper, see own research.

Robert Hooke = observed connection between microscopic structures and colorisation wave nature of light led to conclusion that the cause for the coloration lies in wave interference.

previous

In computer graphics literature, Stam was the first to develop reflection models based on wave optics called diffraction shaders, that can produce colorful diffraction effects. His approach is based on a far field approximation of the Kirchhof integral. He shows that for surfaces representeted as nanoscale heightfieds it is possible to derive their BRDF as the Fourier transformation of a function of the heightfield. Nevetheless, this formulation is not immediately useful for efficent rendering of measured complex nanostructures since this would require the on-the-fly evaluation of and and integration over Fourier transforms of the heightfield that depend on the light and viewing geometry. In his derivations, Stam models heightfields as probabilistic superpositions

of bumps forming periodic like structures. This provides him an analytical identity for this class of heightfields. However, boplogocal nanostructures are way more complex and do not lend themself to this simplified statistical model.

follow ups

1.4   Overview

The reminder of this thesis is organized as the follows: due to the fact that this thesis has a rather advanced mathematical complexity the first part of chapter 2 introduces some important definitions which are required in order to be able to follow the derivaion in the last third of chapter 2. Before starting the derivations a brief summary of J. Stam's Paper about diffraction shaders is provided since this whole thesis is based on his BRDF representation. Our derivations itself are listed step-wiese, whereas there is a final representation provided by the end of chapter 2. Chapter 3 addresses the practical part of this thesis, the implementation of our diffraction model, explaining all precomputation steps and how rendering is preformed in our developed framework for this thesis. Chapter 4 evaluates the validity of our brdf model by rendering the effect of diffraction of a blaze grating for a fixed reflection direction for every indicent directin. Chapter presents the rendering results of our shader for real world paramters, applying our shader on AFM taken snake patches. The thesis is rounded off by providing a conclusion.

2 Theoretical Background

2.1 Definitions

2.1.1 Diffraction

Diffraction refers to various wave-like phenomena which occur when a wave encounters an obstacle, which cannot be modeled using the standard ray theory of light. In classical physics, the diffraction phenomenon is described as the apparent bending of waves around small obstacles and the spreading out of waves past small openings. While diffraction occurs whenever propagating waves encounter such changes, its effects are generally most pronounced for waves whose wavelength is roughly similar to the dimensions of the diffracting objects. This implies diffraction occures mostly when the surface detail is highly anisotropic. If the obstructing object provides multiple, closely spaced openings, a complex pattern of varying intensity can result. This is due to the superposition, or interference, of different parts of a wave that travels to the observer by different paths (see diffraction grating).

Example: Light rays passing through a small aperture will begin to diverge and interfere with one another. This becomes more significant as the size of the aperture decreases relative to the wavelength of light passing through, but occurs to some extent for any aperture or concentrated light source.
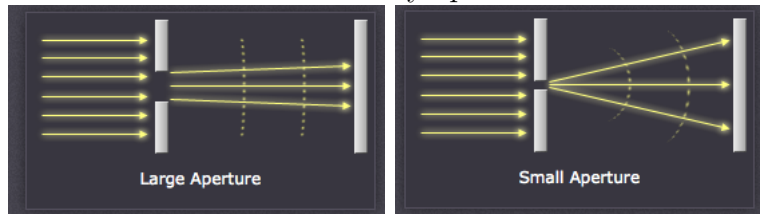
Since the divergent rays now travel different distances, some move out of phase and begin to interfere with each other — adding in some places and partially or completely canceling out in others. This interference produces a diffraction pattern with peak intensities where the amplitude of the light waves add, and less light where they subtract. If one were to measure the intensity of light reaching each position on a line, the measurements would appear as bands similar to those shown below.

Diffraction Pattern
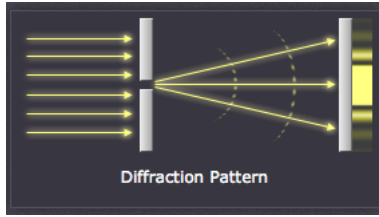
In general interference produces colorful effects due to the phase differences caused by a wave traversing thin media of different indices of refraction.

The effects of diffraction are often seen in everyday life. The most striking examples of diffraction are those that involve light; for example, the closely spaced tracks on a CD or DVD act as a diffraction grating to form the familiar rainbow pattern seen when looking at a disk

In optics, a diffraction grating is an optical component with a periodic structure, which splits and diffracts light into several beams travelling in different directions. The directions of these beams depend on the spacing of the grating and the wavelength of the light so that the grating acts as the dispersive element.

The relationship between the grating spacing and the angles of the incident and diffracted beams of light is known as the grating equation.

FRAUENHOFER DIFFRACTION

2.1.2 Radiometry

Light is fundamentally a propagation form of enegry, so it is useful to define the SI unit of energy which is joule (J). To aid our intuition, let us describe radiometry in terms of collections of large numbers of photons. A photon can be considered as a quantum of light that has a position, direction of propagation and a wavelength λ measured in nanometers. A photon travels in a certain speed, denoted by $v = \frac{c}{n}$, that depends only on the refractive index n of the medium through which it propagates and the speed of light c. This allows us do define the frequency $f = \frac{c}{\lambda}$. The amount of energy q carried by a photon is given by the following relationship: $q = hf = \frac{hc}{\lambda}$ where h is the Plank's constant.

Spectral Energy

If there is a large collection of photons given, their total energy $Q = \sum_i q_i$ is the sum of energies of each photon q_i within the collection. But how is the energy distributed across wavelenghts? One way in order to determine this

distribution is to order all photons by their associated wavelength and then make a histogram from them. This is achieved by a discretization of their spectrum and combine all photons which will fall into the same interval, i.e. compute the sum for each interval from the energy of all their photons. By dividing such an interval by its length, denoted by Q_λ, we get a relatively scaled interval energy, which is called spectral energy and it is an intensive quantity. Intensive quantities can be thought of as density functions that tell the density of an extensive quantity at an infinitesimal point.

Power
Power is the estimated rate of energy production for light sources and is measured in the unit Watts, denoted by Q, which is another name for joules per second. Since power is a density over time, it is well defined even when energy production is varying over time. As with energy, we are really interested in the spectral power, measured in W/nm, denoted by Φ_λ

Irradiance
The term irradiance comes into place when we are interested in *how much light hits a given point.* In order to answer this question, we must make use of a density function. Let ΔA a finite area sensor that is smaller than the light field being measured. The spectral irradiance E is just the power per unit area $\frac{\Delta \Phi}{\Delta A}$ which is

$$E = \frac{\Delta q}{\Delta A \Delta t \Delta \lambda} \tag{1}$$

Thus the units of irradiance are $Jm^{-2}s^{-1}(nm)^{-1}$, the power per unit surface area.

Radiance

TODO: SHOW IMAGE: SOLID angle $WIKI : http : //en.wikipedia.org/wiki/Radiance$ $CGSlides 2012 - 6.shading\ Book : Fundamentals of computer graphics$
Although irradiance tells us how much light is arriving at a point, it tells us little about the direction that light comes from. To measure something similar to what we see with our eyes we need to be able to associate the quantity *how much light with a specific direction.*

Radiance is a measure of the quantity of radiation that passes through or is emitted from a surface and falls within a given solid angle in a specified direction. Think of it as the energy carried along a narrow beam of light. This means radiance characterizes the total emission of reflectance. It indicates how much of the power emitted by a reflecting surface will be received by an optical system looking at the surface from some given angle of view. Formally, this leads us to the following definition of radiance:

$$L(\omega) = \frac{d^2\Phi}{dAd\Omega cos(\theta)} \approx \frac{\Phi}{\Omega A cos(\theta)} \tag{2}$$

where L is the observed radiance in the unit energy per area per solid angle, which is Wm^-2sr^-1 in direction ω which has an angle θ between the surface normal and ω, Θ is the total flux or power emitted, θ is the angle between the surface normal and the specified direction, A is the area of the surface and Ω is the solid angle in the unit steradian subtended by the observation or measurement.

It is useful to distinguish between radiance incident at a point on a surface and exitant from that point. Terms for these concepts sometimes used in the graphics literature are surface radiance L_r for the radiance *reflected* from a surface and field radiance L_i for the radiance *incident* at a surface.

BRDF
The bidirectional reflectance distribution function, in short BRDF, denoted as $f_r(\omega_i, \omega_r)$ is a four dimensional function that defines *how light is reflected at an opaque surface*. The function takes a negative directed incoming light direction, ω_i, and outgoing direction, ω_r as input argument. Both are defined with respect to the surface normal **n**.Hence A BRDF returns the ratio of reflected radiance exiting along ω_r to the irradiance incident on the surface from direction ω_i, which is formally:

$$BRDF(\omega_i, \omega_r) = f_r(\omega_i, \omega_r) \tag{3}$$

$$= \frac{dL_r(\omega_r)}{dE_i(\omega_i)} \tag{4}$$

$$= \frac{dL_r(\omega_r)}{L_i(\omega_i)cos(\theta_i)d\omega_i} \tag{5}$$

L is the reflected radiance, E is the irradiance and θ_i is the angle between ω_i and the surface normal, **n**. The index i indicates incident light, whereas the index r indicates reflected light.

Spectral Rendering

In Computer Graphics, spectral rendering is where a scene's light transport is modeled considering the whole span of wavelengths instead of R,G,B values (still relating on geometric optic, which ignore wave phase). The motivation is that real colors of the physical world are spectrum; trichromatic colors are only inherent to Human Visual System.

In Computer Graphics, when talking about Spectral Rendering, we are refering to use the whole span of wavelengths instead just using RGB values in order for rendering a scene's light transport. The motivation for using the whole wavelength spectrum is due to the fact that trichromatic colors are only inherent to human visual system and therefore many phenomenons are poorly represented just using trichromy.

Color spaces

In order to see how crucial the role human vision plays, we only have to look the the definition of color: *Color is the aspect of visual perception by which an observer may distinguish differences between two structure-free filds of view of the same size and shape such as may be caused by differences in the spectral composition of the radiant energy concerned in the oberservation.* - Wyszechki and Siles, 2000 mentioned in Computer Graphics Fundamentals Book.

Each color can be represented by three numbers, for instance defined by (X,Y,Z) tristimulus values. However, its primaries are imaginary, meanung that is is not possible to construct a device that has three light sources (all positive) that can reprodue all colors in the visible spectrum. A large number of (X,Y,Z) values do not even correspond to a phyisical color.

CIE 1931 RGB and CIE 1931 XYZ color spaces are the first mathematical-ly defined color spaces. They were created by the International Commission on Illumination (CIE) in 1931.

The CIE's color matching functions $\overline{x}(\lambda)$, $\overline{y}(\lambda)$ and $\overline{z}(\lambda)$ are the numerical description of the chromatic response of the observer (described above). They can be thought of as the spectral sensitivity curves of three linear light detectors yielding the CIE tristimulus values X, Y and Z. Collectively, these

three functions are known as the CIE standard observer.[9]

The tristimulus values for a color with a spectral power distribution $I(\lambda)$, are given in terms of the standard observer by:

$$X = \int_{380}^{780} I(\lambda)\,\bar{x}(\lambda)\,d\lambda$$

$$Y = \int_{380}^{780} I(\lambda)\,\bar{y}(\lambda)\,d\lambda$$

$$Z = \int_{380}^{780} I(\lambda)\,\bar{z}(\lambda)\,d\lambda$$

where λ, is the wavelength of the equivalent monochromatic light (measured in nanometers).

It is not possible to build a display that corresponds to CIE XYZ, for this reasons it is necessary to design other color spaces, which are phyiscal realizable, offers efficient encoding, are perceptual uniform and have an intuitive color specification.

There are simple conversions between XYZ color space to any other color space defined, as linear transfromations.

2.1.3 Signal Processing Basics

A signal is a function that conveys information about the behavior or attributes of some phenomenon. In the physical world, any quantity exhibiting variation in time or variation in space (such as an image) is potentially a signal that might provide information on the status of a physical system, or convey a message between observers

Fourier Transformation
The Fourier-Transform is a mathematical tool which allows to transform a given function or rather a given signal from defined over a time- (or spatial-) domain into its corresponding frequency-domain.

Let f an measurable function over $\mathbb{R}^n$. Then, the continnous Fourier Transformation(**FT**), denoted as $\mathcal{F}\{f\}$ of f is defined as, ignoring all constant factors in the formula:

$$\mathcal{F}_{FT}\{f\}(w) = \int_{\mathbb{R}^n} f(x)e^{-iwt}dt \tag{6}$$

12

whereas its inverse transform is defined like the following which allows us to obtain back the original signal:

$$\mathcal{F}_{FT}^{-1}\{f\}(w) = \int_{\mathbb{R}} \mathcal{F}\{w\}e^{iwt}dt \tag{7}$$

An usual identity for w is the the so called angular with $w = \frac{2\pi}{T} = 2\pi v_f$ where T is the period, v_f the frequency.

By using Fourier Analysis, which is the approach to approximate any function by sums of simpler trigonometric functions, we gain the so called Discrete Time Fourier Transform (in short **DTFT**). The DTFT operates on a discrete function. Usually, such an input function is often created by digitally sampling a continnous function. The DTFT itself is operation on a discretized signal on a continnous, periodic frequency domain and looks like the following:

$$\mathcal{F}_{DTFT}\{f\}(w) = \sum_{-\infty}^{\infty} f(x)e^{-iwk} \tag{8}$$

We can further discretize the frequency domain and will get then the Discrete Fourier Transformation (in short **DFT**) of the input signal:

$$\mathcal{F}_{DFT}\{f\}(w) = \sum_{n=0}^{N-1} f(x)e^{-iw_n k} \tag{9}$$

Where the angular frequency w_n is defined like the following $w_n = \frac{2\pi n}{N}$ and N is the number of samples within an equidistant periode sampling.

Convolution
The convolution $f * g$ of two functions $f, g \colon \mathbb{R}^n \to \mathbb{C}$ is defined as:

$$(f * g)(t) = \int_{\mathbb{R}^n} f(t)g(t-x)dx \tag{10}$$

Note that the Fourier transform of the convolution of two functions is the product of their Fourier transforms. This is equivalent to the fact that Convolution in spatial domain is equivalent to multiplication in frequency domain. Therefore, the inverse Fourier transform of the product of two Fourier transforms is the convolution of the two inverse Fourier transforms

Taylor Series

Taylor series is a representation of a function as an infinite sum of terms that are calculated from the values of the function's derivatives at a single point.

The Taylor series $\mathcal{T}$ of a real or complex-valued function f(x) that is infinitely differentiable at a real or complex number a is the power series:

$$\mathcal{T}(f;a)(x) = \sum_{n=0}^{\infty} \frac{f^n(a)}{n!}(x-a)^n \tag{11}$$

2.2 Thesis Basis: J.Stam's Paper about Diffraction Shader

GOAL main task in the theory of diffraction is to solve this wave equation for different geometries. we are interested in computing the reflected waves from various types of surfaces

abstract: before: most reflection models empirically or based on ray-theory of light. now: new reflection model based on wave theory modeling the effect of diffraction

In his Paper Diffraction Shader, Jos Stam derives a BRDF which modeling the effect of diffraction for various analytical anistropic reflaction models using the scalar Kirchof theory and the theory of random processes. By employing the so called scalar wave theory of diffraction [source 5 in stams paper] in which a wave is assumed to be a complex valued scalar. It's noteworthy, that stam's BRDF formulation does not take into account the polarization of the light. Fortunately, light sources like sunlight and light bulbs are unpilarizaed. In our simulations we will always assume we have given i directional light source, i.e. sunlight. Hence, we can use stam's model for our derivations

A further assumption in Stam's Paper is, the emanated waves from the source are stationary, which implies the wave is a superposition of independent monochromatic waves. This implies that each wave is associated to a definite wavelangth lambda. However, sunlight once again fulfills this fact.

Mention Helmolth equation, which has the solution $k = \frac{2\pi}{\lambda}$ which is the wavenumber

Based on his these previous assumptions and applying Stam starts his derviations by applying the so called Kirchhoff integral, which is relating the reflected field to the incoming field. This equation is a formalization of Huygen's well-known principle that states that if one knows the wavefront at a given moment, the wave at a later time can be deduced by considering

14

each point on the first wave as the source of a new disturbance, i.e. once the field $\psi_1 = e^{ik\mathbf{x}\cdot\mathbf{ss}}$ on the surface is known, the field everywhere ψ_2 else away from the surface can be computed. More precisely, we want to compute the wave ψ_2 equal to the reflection of an incoming planar monochromatic wave $\psi_1 = e^{ik\omega_i * x}$ traveling in the direction ω_i from a surface S to the light source. Mathematically this can be formulized the following:

$$\psi_2 = \frac{ike^{iKR}}{4\pi R}(F\mathbf{v} - \mathbf{p}) \cdot \int_S \hat{\mathbf{n}}e^{ik\mathbf{v}\cdot\mathbf{s}d\mathbf{s}} \tag{12}$$

In applied optics, when dealing with scattered waves, one does use differential scattering cross-section rather than defining a BRDF which has the following identitiy:

$$\sigma^0 = 4\pi \lim_{R\to\infty} R^2 \frac{\langle|\psi_2|^2\rangle}{\langle|\psi_1|^2\rangle} \tag{13}$$

Relationship between the BRDF and the scattering cross section is the follwing:

The relationship between the BRDF and the scattering cross section can be shown to be equal to $BRDF = \frac{1}{4\pi}\frac{1}{A}\frac{\sigma^0}{cos(\theta_i)cos(\theta_r)}$ Wheras θ_i and θ_r are the angles that the vectors $-\omega_i$ and ω_r make with the vertical direction.
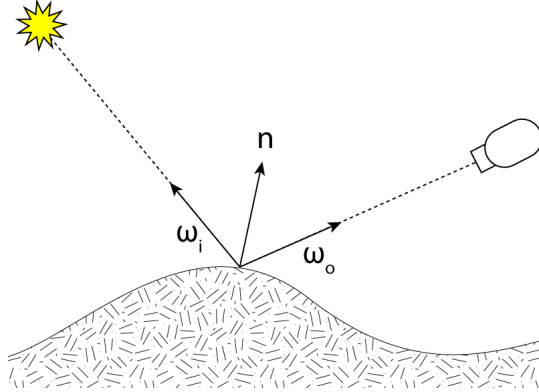
where R is the distance from the center of the patch to the receiving point x_p, $\hat{\mathbf{n}}$ is the normal of the surface at s and the vectors:

$$\mathbf{v} = -\omega_i - \omega_r = (u, v, w)$$

$$\mathbf{p} = -\omega_i + \omega_r$$

15

During his derivations, Stam provides a analytical representation for the Kirchhoff integral by using his assumptions. He restricts himself to the reflaction of waves from height fields $h(x, y)$ with the assumption that the surface is defined as an elevation over the (x,y) plane using the surface plane approximation.

Which will lead him to the follwoing identity for the Kirchhoff integral

$$\mathbf{I}(ku, kv) = \int \int \frac{1}{ikw}(-p_x, -p_y, ikwp) \tag{14}$$

wheras stam formulates for a hightfield auxilary function $p(x, y) = e^{iwkh(x,y)}$ where $w = -(cos(\theta_i) + cos(\theta_r))$ and θ_i and θ_r are the angles of incident and reflected directions with the surface normal (ADD picture) and the wavenumber $k = \frac{2\pi}{\lambda}$

$$p(x, y) = e^{ikwh(x,y)} \tag{15}$$

We the observation that the integral is a Fourier transform by $-iku$ and $-ikv$ which will lead us to his final derivation, using the identity of BRDF, and computing the limes:

$$BRDF_\lambda(\omega_i, \omega_r) = \frac{k^2 F^2 G}{4\pi^2 A w^2} \langle |P(ku, kv)|^2 \rangle \tag{16}$$

$BRDF_\lambda(\omega_i, \omega_r)$ is BRDF where wavelength λ ω_i and ω_r are incident and reflected normalized directions vectors, pointing away from the given surface. Which can be written, using the fourier transform (FT) $P(u, v) = F(p)(u, v)$, as: $BRDF_\lambda(\omega_i, \omega_r) = \frac{F^2 G}{\lambda^2 A w^2} abs(P(\frac{u}{\lambda}, \frac{v}{\lambda}))^2$ where F represents the Fresnel term, uv,v,w are derived from the incident and reflected directions as $(u, v, w) = -\omega_i - \omega_r$, abs(P) represents the expected valuess of a random variable X and A is an area of integration on the surface that is considered to contribute to diffraction, G is the geometry term which is $G = \frac{(1+\omega_i \cdot \omega_r)^2}{cos(\theta_i)cos(\theta_r)}$

and P(x,y) is the Fourier transform (FT) of the function p(x,y) from above. This identitiy for the BRDF is the starting point for our derivations.

2.3 Derivations

2.3.1 BRDF formulation

Lets assume we have given an incoming light source with solid angle ω_i, θ_i is its angle of incidence, ω_r is the solid angle for the reflected light, λ wavelength, Ω is the hemisphre we of integration for the incomming light. Then, we are able to formulate a BRDF by using its definiton:

$$f_r(\omega_i, \omega_r) = \frac{dL_r(\omega_r)}{L_i(\omega_i)cos(\theta_i)d\omega_i}$$

$$=> f_r(\omega_i, \omega_r)L_i(\omega_i)cos(\theta_i)d\omega_i = dL_r(\omega_r)$$

$$=> \int_\Omega f_r(\omega_i, \omega_r)L_i(\omega_i)cos(\theta_i)d\omega_i = \int_\Omega dL_r(\omega_r)$$

$$=> L_r(\omega_r) = \int_\Omega f_r(\omega_i, \omega_r)L_i(\omega_i)cos(\theta_i)d\omega_i$$

The last equation is the so called rendering equation. We assume further, that our incident light is a directional, unpolarized light source like sunlight and therefore its radiance is given as

$$L_\lambda(\omega) = I(\lambda)\delta(\omega - \omega_i) \tag{17}$$

where $I(\lambda)$ is the intensity of the relative spectral power for the wavelength λ. Since all light rays are parallel whenever we are provided by a directional light source and we can think of radiance as a measure of the light emitted from a particular surface location into a particular direction, above's radiance identity will follow immediately. By plugging this identity into our current rendering equation, we will get:

$$L_\lambda(w_r) = \int_\Omega BRDF_\lambda(\omega_i, \omega_r)L_\lambda(\omega_i)cos(\theta_i)d\omega_i \tag{18}$$

$$= BRDF_\lambda(\omega_i, \omega_r)I(\lambda)cos(\theta_i) \tag{19}$$

where $L_\lambda(\omega_i)$ is the incomming radiance and $L_\lambda(\omega_r)$ is the radiance reflected by given surface Note that above's integral vanishes since $\delta(\omega - \omega_i)$ is only equal one if and only if $\omega = \omega_i$.

For the $BRDF(\omega_i, \omega_r)$ we are going to use Stam's main derivation (16) applying the fact that the wavenumber is equal $k = \frac{2\pi}{\lambda}$:

$$BRDF(\omega_i, \omega_r) = \frac{k^2 F^2 G}{4\pi^2 A w^2} \langle |P(ku, kv)|^2 \rangle$$

$$= \frac{k^2 F^2 (1 + \omega_i \cdot \omega_r)^2}{cos(\theta_i)cos(\theta_r)4\pi^2 A w^2} \langle |P(ku, kv)|^2 \rangle$$

$$= \frac{4\pi^2 F^2 (1 + \omega_i \cdot \omega_r)^2}{cos(\theta_i)cos(\theta_r)4\pi^2 A \lambda^2 w^2} \langle |P(ku, kv)|^2 \rangle$$

$$= \frac{F(w_i, w_r)^2 (1 + \omega_i \cdot \omega_r)^2}{cos(\theta_i)cos(\theta_r)A \lambda^2 w^2} \langle |P(ku, kv)|^2 \rangle$$

going back to the definition of $(u, v, w) = -\omega_i - \omega_r$ and using spherical coordinates, we get for w the following identity $w = -\omega_i - \omega_r = -(\omega_i + \omega_r) = -(cos(\theta_i) + cos(\theta_r))$ and therefore w^2 is equal $(cos(\theta_i) + cos(\theta_r))^2$ This new fact will allow us to get even further:

$$L_\lambda(\omega_r) = \frac{F(\omega_i, \omega_r)^2 (1 + \omega_i \cdot \omega_r)^2}{A \lambda^2 cos(\theta_i)cos(\theta_r)(cos(\theta_i) + cos(\theta_r))^2} \langle \left| P_{cont}(\frac{2\pi u}{\lambda}, \frac{2\pi v}{\lambda}) \right|^2 \rangle cos(\theta_i)I(\lambda)$$

$$= I(\lambda) \frac{F(\omega_i, \omega_r)^2 (1 + \omega_i \cdot \omega_r)^2}{\lambda^2 A (cos(\theta_i) + cos(\theta_r))^2 cos(\theta_r)} \langle \left| P_{cont}(\frac{2\pi u}{\lambda}, \frac{2\pi v}{\lambda}) \right|^2 \rangle$$

$$= I(\lambda) \frac{F(\omega_i, \omega_r)^2 (1 + \omega_i \cdot \omega_r)^2}{\lambda^2 A (cos(\theta_i) + cos(\theta_r))^2 cos(\theta_r)} \langle \left| T_0^2 P_{dtft}(\frac{2\pi u}{\lambda}, \frac{2\pi v}{\lambda}) \right|^2 \rangle$$

P_{cont} denotes the continuous inverse Fourier-Transform for the Taylor-Series of our heightfield representing the nano-scaled surface structure, i.e. $P(k, l) = \mathcal{F}^{-1}\{p\}(k, l)$ and P_{dtft} is the inverse Discrete Time Fourier Transform of $p(x, y) = e^{ikwh(x,y)}$. Furthermore T_0 the sampling distance for the discretization of $p(x, y)$ assuming equal and uniform sampling in both dimensions x, y.

2.3.2 Relative BRDF

In this section we are going to explain how to scale our BRDF formulation such that all of its possible output values are mapped into the range $[0, 1]$. Such a relative BRDF formulation will ease our life for later rendering

puposes since usually color values are within the range $[0, 1]$, too. Furthermore, this will allow us to properly blend the resulting illumination caused by diffraction with a texture map.

Let us examine what $L_\lambda(\omega_r)$ will be for $\omega_r = \omega_0 := (0, 0, *)$ i.e. specular reflection case, denoted as $L_\lambda^{spec}(\omega_0)$.

When we know the expression for $L_\lambda^{spec}(\omega_0)$ we would be able to compute the relative reflected radiance for our problem by simply dividing $L_\lambda(\omega_r)$ by $L_\lambda^{spec}(\omega_0)$, denoted as

$$\rho_\lambda(\omega_i, \omega_r) = \frac{L_\lambda(\omega_r)}{L_\lambda^{spec}(\omega_0)} \tag{20}$$

But first, let us derive the following expression:

$$L_\lambda^{spec}(\omega_0) = I(\lambda) \frac{F(\omega_0, \omega_0)^2 (1 + \begin{pmatrix} 0 \\ 0 \\ 1 \end{pmatrix} \cdot \begin{pmatrix} 0 \\ 0 \\ 1 \end{pmatrix})^2}{\lambda^2 A (cos(0) + cos(0))^2 cos(0)} \langle \left| T_0^2 P_{dtft}(0, 0) \right|^2 \rangle$$

$$= I(\lambda) \frac{F(\omega_0, \omega_0)^2 (1 + 1)^2}{\lambda^2 A (1 + 1)^2 1} \left| T_0^2 N_{sample} \right|^2$$

$$= I(\lambda) \frac{F(\omega_0, \omega_0)^2}{\lambda^2 A} \left| T_0^2 N_{sample} \right|^2$$

Where $N_{samples}$ is the number of samples of the DTFT.

Thus, we can plug our last derived expression into the definition for the relative reflectance radiance in the direction w_r and will get:

$$\rho_\lambda(\omega_i, \omega_r) = \frac{L_\lambda(\omega_r)}{L_\lambda^{spec}(\omega_0)}$$

$$= \frac{I(\lambda) \frac{F(\omega_i, \omega_r)^2 (1 + \omega_i \cdot \omega_r)^2}{\lambda^2 A (cos(\theta_i) + cos(\theta_r))^2 cos(\theta_r)} \langle \left| T_0^2 P_{dtft}(\frac{2\pi u}{\lambda}, \frac{2\pi v}{\lambda}) \right|^2 \rangle}{I(\lambda) \frac{F(\omega_0, \omega_0)^2}{\lambda^2 A} \left| T_0^2 N_{sample} \right|^2}$$

$$= \frac{F^2(\omega_i, \omega_r)(1 + \omega_i \cdot \omega_r)^2}{F^2(\omega_0, \omega_0)(cos(\theta_i) + cos(\theta_r))^2 cos(\theta_r)} \langle \left| \frac{P_{dtft}(\frac{2\pi u}{\lambda}, \frac{2\pi v}{\lambda})}{N_{samples}} \right|^2 \rangle$$

for simplification and a better overview, let us introduce the following expression, the so called gain-factor:

$$C(\omega_i, \omega_r) = \frac{F^2(\omega_i, \omega_r)(1 + \omega_i \cdot \omega_r)^2}{F^2(\omega_0, \omega_0)(cos(\theta_i) + cos(\theta_r))^2 cos(\theta_r) N^2_{samples}} \tag{21}$$

Using this substitute, we will end up with the following expression for the relative reflectance radiance:

$$\rho_\lambda(\omega_i, \omega_r) = C(\omega_i, \omega_r) \langle \left| P_{dtft}(\frac{2\pi u}{\lambda}, \frac{2\pi v}{\lambda}) \right|^2 \rangle \tag{22}$$

Using the previous definition for the relative reflectance radiance

$$\rho_\lambda(\omega_i, \omega_r) = \frac{L_\lambda(\omega_r)}{L^{spec}_\lambda(\omega_0)} \tag{23}$$

which we can rearrange to the expression

$$L_\lambda(\omega_r) = \rho_\lambda(\omega_i, \omega_r) L^{spec}_\lambda(\omega_0) \tag{24}$$

Let us choose $L^{spec}_\lambda(w_0) = S(\lambda)$ such that is has the same profile as the relative spectral power distribution of CIE Standard Illuminant $D65$. Further, when integration over λ for a specular surface we should get CIE_{XYZ} values corresponding to the white point for $D65$ The corresponding tristimulus values using CIE colormatching functions for the CIE_{XYZ} values look like:

$$X = \int_\lambda L_\lambda(\omega_r)\overline{x}(\lambda)d\lambda \tag{25}$$

$$Y = \int_\lambda L_\lambda(\omega_r)\overline{y}(\lambda)d\lambda \tag{26}$$

$$Z = \int_\lambda L_\lambda(\omega_r)\overline{z}(\lambda)d\lambda \tag{27}$$

where $\overline{x}$, $\overline{y}$, $\overline{z}$ are the color matching functions

Using our last finding for $L_\lambda(\omega_r)$ with the definition for the tristimulus values we can actually derive an expression for computing the colors for our BRDF formula. Since X, Y, Z are defined similarly, it satisfies to derive an explicit expression for just one tristimulus term, for example X. The other two will look the same, except the we have to replace all X with Y or Z respectively. Therefore, we get:

$$X = \int_\lambda L_\lambda(\omega_r)\overline{x}(\lambda)d\lambda$$

$$= \int_\lambda \rho_\lambda(\omega_i, \omega_r)L_\lambda^{spec}(\omega_0)\overline{x}(\lambda)d\lambda$$

$$= \int_\lambda \rho_\lambda(\omega_i, \omega_r)S(\lambda)\overline{x}(\lambda)d\lambda$$

$$= \int_\lambda C(\omega_i, \omega_r)\langle\left|P_{dtft}(\frac{2\pi u}{\lambda}, \frac{2\pi v}{\lambda})\right|^2\rangle S(\lambda)\overline{x}(\lambda)d\lambda$$

$$= C(\omega_i, \omega_r)\int_\lambda \langle\left|P_{dtft}(\frac{2\pi u}{\lambda}, \frac{2\pi v}{\lambda})\right|^2\rangle S(\lambda)\overline{x}(\lambda)d\lambda$$

$$= C(\omega_i, \omega_r)\int_\lambda \langle\left|P_{dtft}(\frac{2\pi u}{\lambda}, \frac{2\pi v}{\lambda})\right|^2\rangle S_x(\lambda)d\lambda$$

Where we used the definition $S_x(\lambda)\overline{x}(\lambda)$ in the last step.

2.3.3   Taylor approximation for BRDF

In this section, we will show there is an approximation for the inverse Fourier Tranformation of Stam's auxilary function p(x,y). This derivation will rely on the definition of Taylor Series expansion and will further provide an error bound for our approximation approach. Last, we will extend our last findings by the findings derived within this section and get a new identity for our relative BRDF representation.

Given $p(x, y) = e^{ikwh(x,y)}$ form Stam's Paper where h(x,y) is a given heightfield. Let be y real or even complex value, and lets consider the power series for the the exponential function

$$e^t = 1 + t + \frac{t^2}{2!} + \frac{t^3}{3!} + ... = \sum_{n=0}^\infty \frac{t^n}{n!}$$

Let us define $t := t(x, y) = ikwh(x, y)$ where i is the imaginary number. For simplification, let us denote $h(x, y)$ as h. Then it follows by our previous stated identities:

$$e^t = 1 + (ikwh) + \frac{1}{2!}(ikwh)^2 + \frac{1}{3!}(ikwh)^3 + \dots$$
$$= \sum_{n=0}^{\infty} \frac{(ikwh)^n}{n!}.$$

Hence it holds $p(x,y) = \sum_{n=0}^{\infty} \frac{(ikwh(x,y))^n}{n!}$.
Let us now compute the Fourier Transformation of p(x,y) form above:

$$\mathcal{F}\{p\}(u,v) = \mathcal{F}\left\{ \sum_{n=0}^{\infty} \frac{(ikwh)^n}{n!}. \right\}(u,v)$$

$$=^{\mathcal{F} \, lin \, Operator} \sum_{n=0}^{\infty} \mathcal{F}\left\{ \frac{(ikwh)^n}{n!} \right\}(u,v)$$

$$= \sum_{n=0}^{\infty} \frac{(ikw)^n}{n!} \mathcal{F}\{h^n\}(u,v)$$

Hence it follows: $P(\alpha, \beta) = \sum_{n=0}^{\infty} \frac{(ikw)^n}{n!} \mathcal{F}\{h^n\}(\alpha, \beta)$ for which $\mathcal{F}_{FT}\{h^n\}(u,v)$.
Next we are going to look for an $N \in \mathbb{N}$ such that

$$\sum_{n=0}^{N} \frac{(ikwh)^n}{n!} \mathcal{F}\{h^n\}(\alpha, \beta) \approx P(\alpha, \beta)$$

is a good approximation. But first the following two facts have to be proven:

1. Show that there exist such an $N \in \mathbb{N}$ s.t the approximation holds true.

2. Find a value for B s.t. this approximation is below a certain error bound, for example machine precision ϵ.

Proof Sketch of 1.

By the **ratio test** (see [1]) It is possible to show that the series $\sum_{n=0}^{N} \frac{(ikwh)^n}{n!} \mathcal{F}\{h^n\}(\alpha, \beta)$ converges absolutely:
Proof: Consider $\sum_{k=0}^{\infty} \frac{y^n}{n!}$ where $a_k = \frac{y^k}{k!}$. By applying the definition of the ratio test for this series it follows:

$$\forall y : limsup_{k \to \infty} |\frac{a_{k+1}}{a_k}| = limsup_{k \to \infty} \frac{y}{k+1} = 0$$

Thus this series converges absolutely, no matter what value we will pick for y.

Part 2: Find such an N

Let $f(x) = e^x$. We can formulate its Taylor-Series, stated above. Let $P_n(x)$ denote the n-th Taylor-Polinomial,

$$P_n(x) = \sum_{k=0}^{n} \frac{f^{(k)}(a)}{k!}(x-a)^k$$

where a is our developing point (here a is equal zero).

We can define the error of the n-th Taylor-Polinomial to be $E_n(x) = f(x) - P_n(x)$. the error of the n-th Taylor-Polinomial is difference between the value of the function and the Taylor polinomial This directly implies $|E_n(x)| = |f(x) - P_n(x)|$. By using the Lagrangien Error Bound - (see source [2]) it follows: $|E_n(x)| \leq \frac{M}{(n+1)!}|x-a|^{n+1}$ with a=0, where **M** is some value satisfying $|f^{(n+1)}(x)| \leq M$ on the interval $I = [a, x]$. Since we are interested in an upper bound of the error and since **a** is known, we can reformulate the interval as $I = [0, x_{max}]$, where

$$x_{max} = \|i\| k_{max} w_{max} h_{max}$$

since we are interested in computing an error bound for $e^{ikwh(x,y)}$. From Stam's Paper we know some paramters for the length, width and height for a given sample patch, i.e. heightfield h(x,y) and when using those parameters are able to find a explicit number for x_{max}.

Facts we are using from Stam's Paper:

- Height of bump: 0.15micro meters

- Width of a bump: 0.5micro meters

- Length of a bump: 1micro meters

- $k = \frac{2\pi}{\lambda}$ is the wavenumber and $\lambda \in [\lambda_{min}, \lambda_{max}]$ its wavelength hence $k_{max} = \frac{2\pi}{\lambda_{min}}$

- w is a component of the vector $\vec{v} = \vec{k_1} - \vec{k_2} = (u, v, w)$, where $\vec{k_1}$ and $\vec{k_2}$ are **normalized** direction vectors and this each component can have a value in range [-2, 2].

- for simplification, assume$[\lambda_{min}, \lambda_{max}] = [400nm, 700nm]$.

Hence

$$
\begin{aligned}
x_{max} &= \|i\| * k_{max} * w_{max} * h_{max} \\
&= k_{max} * w_{max} * h_{max} \\
&= 2 * \left(\frac{2\pi}{4 * 10^{-7}m}\right) * 1.5 * 10^{-7} \\
&= 1.5\pi
\end{aligned}
$$

and it follows for our intervall $I = [0, 1.5\pi]$.

Next we are going to find the value for M. Since the exponential function is monoton growing (on the interval I) and and the derivative of the **exp** function is the exp function itself, we can find such an M:

$$
\begin{aligned}
M &= e^{x_{max}} \\
&= exp(1.5\pi)
\end{aligned}
$$

and $|f^{(n+1)}(x)| \leq M$ holds. With

$$
\begin{aligned}
|E_n(x_{max})| &\leq \frac{M}{(n+1)!} |x_{max} - a|^{n+1} \\
&= \frac{exp(1.5\pi) * (1.5\pi)^{n+1}}{(n+1)!}
\end{aligned}
$$

we now can find a value of n for a given bound, i.e. we can find an value of $N \in \mathbb{N}$ s.t. $\frac{exp(1.5\pi)*(1.5\pi)^{N+1}}{(N+1)!} \leq \epsilon$. With Octave/Matlab we can see:

- if N=20 then $\epsilon \approx 2.9950 * 10^{-4}$

- if N=25 then $\epsilon \approx 8.8150 * 10^{-8}$

- if N=30 then $\epsilon \approx 1.0050 * 10^{-11}$

Conclusion   With this approach we have that $\sum_{n=0}^{25} \frac{(ikwh)^n}{n!} \mathcal{F}\{h^n\}(\alpha, \beta)$ is an approximation of $P(u, v)$ with error $\epsilon \approx 8.8150 * 10^{-8}$. This means we can precompute 25 Fourier Transformations (for example via FFT2) and then sum them up in order to approximate P(u,v) and $\epsilon \approx 8.8150 * 10^{-8}$.

This approach will allow us to speed up our shader. Furthermore we see that when we just take 5 more iterations, we will reduce the error bound to the dimension of 10^{-11}.

Using $P_{dtft} = \mathcal{F}^{-1}\{p\}(u,v)$ definied in the section of the taylor approximationwe get for the tristumulus value X, we will get:

$$X = C(w_i, w_r) \int_\lambda \langle \left| P_{dtft}(\frac{2\pi u}{\lambda}, \frac{2\pi v}{\lambda}) \right|^2 \rangle S_x(\lambda) d\lambda$$

$$= C(w_i, w_r) \int_\lambda \left| \sum_{n=0}^{N} \frac{(wk)^n}{n!} \mathcal{F}^{-1}\{i^n h^n\}(\frac{2\pi u}{\lambda}, \frac{2\pi v}{\lambda}) \right|^2 S_x(\lambda) d\lambda$$

2.3.4 Sampling: Gaussian Window

why this identity works: The DFT of a discrete heightfield patch is equivalent to the DTFT of an infinitely periodic function consisting of replicas of the same discrete patch. By windowing with a window function that is zero outside the central replica, the convolution of either the DFT or the DTFT of heightfield with the fourier transfrom of the window becomes equivalent.

Let $window_g$ denote the gaussian window with $4\sigma_s$ μm where $\sigma_f = \frac{1}{2\pi\sigma_s}$ let us further substitute $\mathbf{t}(\mathbf{x}, \mathbf{y}) = i^n h(x,y)^n$

$$\mathcal{F}_{dtft}^{-1}\{\mathbf{t}\}(u,v) = \mathcal{F}_{fft}^{-1}\{\mathbf{t}\}(u,v) window_g(\sigma_f) \tag{28}$$

Therefore we can deduce the following expression from this:

$$\mathcal{F}_{dtft}^{-1}\{\mathbf{t}\}(u,v) = \int_{-\infty}^{\infty} \int_{-\infty}^{\infty} F_{fft}^{-1}\{\mathbf{t}\}(w_u, w_v)\phi(u - w_u, v - w_v)dw_u dw_v$$

$$= \int_{-\infty}^{\infty} \int_{-\infty}^{\infty} \sum_i \sum_j F_{fft}^{-1}\{\mathbf{t}\}(w_u, w_v)$$

$$\delta(w_u - w_i, w_v - w_j)\phi(u - w_u, v - w_v)dw_u dw_v$$

$$= \sum_i \sum_j \int_{-\infty}^{\infty} \int_{-\infty}^{\infty} F_{fft}^{-1}\{\mathbf{t}\}(w_u, w_v)$$

$$\delta(w_u - w_i, w_v - w_j)\phi(u - w_u, v - w_v)dw_u dw_v$$

$$= \sum_i \sum_j F_{fft}^{-1}\{\mathbf{t}\}(w_u, w_v)\phi(u - w_u, v - w_v)$$

where

$$\phi(x,y) = \pi e^{-\frac{x^2+y^2}{2\sigma_f^2}} \tag{29}$$

2.3.5 Aplitude smooting

Let us consider the so called 1-dimensional Box-function with length T which is defined as the following: ADD AN IMAGE OF BOXFUNCTION

$$Box(x) = \begin{cases} 1 & \text{if } x \leq T \\ 0 & \text{if } else \end{cases}$$

We assume, that our given heighfield can be represented as a 2-dimensional box-function. Note that we can use any explicit given constrainted 2-dimensional function and will get some identities like we get from the box-function.

Further we are assuming that we can model the overall surface be assuming this heighfield being distributed in a periodic manor. Therfore, the whole surface can be represented like this $f(x) = \sum_{n=0}^{N} Box(x + nT_1, y + mT_2)$ assuming the given heighfield has the dimensions T_1 by T_2. But let us first consider the 1-dimensional Box-function case before deriving an identity for the Fourier transform of our 2-dimensional Box-function, i.e. the fourier transform of our heighfield.

Note: A function f periodic with periode T means: $\forall x \in \mathcal{R} : Box(x) = Box(x + T)$

A so called bump can be represented by our 1-dimensional Box-function. We assume periodicity which is equaivalent to: $f(x) = \sum_{n=0}^{N} Box(x + nT)$

We are insterested in the 1-dimensional inverse Fourier transform of the 1-dimensional Box-function:

$$\mathcal{F}^{-1}\{f\}(w) = \int f(x)e^{iwx}dx$$

$$= \int_{-\infty}^{\infty} \sum_{n=0}^{N} Box(x + nT)e^{iwx}dx$$

$$= \sum_{n=0}^{N} \int_{-\infty}^{\infty} Box(x + nT)e^{iwx}dx$$

Next, apply the following substituation $x + nT = y$ which will lead us to:

26

$$x = y - nT$$
$$dx = dy$$

Plugging this substituation back to the equation from above we will get

$$\mathcal{F}^{-1}\{f\}(w) = \int f(x)e^{iwx}dx$$

$$= \sum_{n=0}^{N} \int_{-\infty}^{\infty} Box(y)e^{iw(y-nT)}dy$$

$$= \sum_{n=0}^{N} e^{-iwnT} \int_{-\infty}^{\infty} Box(y)e^{iwy}dy$$

$$= \sum_{n=0}^{N} e^{-iwnT} \mathcal{F}\{f\}(w)$$

$$= \mathcal{F}^{-1}\{f\}(w) \sum_{n=0}^{N} e^{-iwnT}$$

We used the fact that the term e^{-iwnT} is a constant when integrating along dy and the identity for the inverse Fourier transform of the Box function. Next, let us consider $\sum_{n=0}^{N} e^{-uwnT}$ further:

$$\sum_{n=0}^{N} e^{-uwnT} = \sum_{n=0}^{N} (e^{-uwT})^n$$

$$= \frac{1 - e^{iwT(N+1)}}{1 - e^{-iwT}}$$

We recognize the geometric series identity for the left-handside of this equation. Since our series is bounded we can derive our right-handside.

Since e^{-ix} is a complex number and every complex number can be written in its polar form, i.e. $e^{-ix} = cos(x) + isin(x)$ we can go even further, using the trigonometric idententities that $cos(-x) = cos(x)$ and $sin(-x) = -sin(x)$:

$$\frac{1 - e^{iwT(N+1)}}{1 - e^{-iwT}} = \frac{1 - cos(wT(N+1)) + isin(wT(N+1))}{1 - cos(wT) + isin(wT)}$$

Which is still a complex number $(p + iq)$. Every complex number can be written as a fraction of two complex numbers. This means that the complex number $(p + iq)$ can be written as $(p + iq) = \frac{(a+ib)}{(c+id)}$ for any $(a + ib), (c + id) \neq 0$. For our case, let us use the follwoing substituations:

$$a := 1 - cos(wT(N+1)) \qquad\qquad b = sin(wT(N+1)) \qquad (30)$$
$$c = 1 - cos(wT) \qquad\qquad d = sin(wT) \qquad (31)$$

hence it follows $\frac{1 - e^{iwT(N+1)}}{1 - e^{-iwT}} = \frac{(a+ib)}{(c+id)}$. By rearanging the terms it follows $(a + ib) = (c + id)(p + iq)$ and multiplying the right handside out we get the follwing system of equations:

$$(cp - dq) = a \qquad\qquad (32)$$
$$(dp + cq) = b \qquad\qquad (33)$$

Which gives lead us we some further math (trick: mult first eq. by c and 2nd by d, then adding them together. using distributivity and we have the identity for p for example, similar for q) to

$$p = \frac{(ac + bd)}{c^2 + d^2} \qquad\qquad (34)$$
$$q = \frac{(bc + ad)}{c^2 + d^2} \qquad\qquad (35)$$

Putting our substituation for a, b, c, d back into the current representatio for p and q and using some trigonometric identites, this we then get:

$$p = \frac{1}{2} + \frac{1}{2}\left(\frac{cos(wTN) - cos(wT(N+1))}{1 - cos(wT)}\right) \qquad (36)$$
$$q = \frac{sin(wT(N+1)) - sin(wTN) - sin(wT)}{2(1 - cos(wT))} \qquad (37)$$

Since we have seen, that $\sum_{n=0}^{N} e^{-uwnT}$ is a complex number and can be written as $(p + iq)$ and we know now the explicit identity for those p and

28

q we get for the 1-dimensional Fourier transform of the 1-dimensional Box-function the following final identity:

$$\mathcal{F}^{-1}\{f\}(w) = \mathcal{F}^{-1}\{f\}(w) \sum_{n=0}^{N} e^{-iwnT}$$
$$= (p + iq)\mathcal{F}^{-1}\{Box\}(w)$$

In oder to derive next a identity for the Fourier transform for our 2-dim heighfield, we can proceed similarly, the only fact which changes is, that we are now in a 2-dimensional domain, i.e. we are about to compute a two-dimensional Fourier transform: Let us again us again a Box-function, this time a 2-dimensional Box-function $Box(x, y)$ just for the sake of convenience.

$$\mathcal{F}^{-1}\{f\}(w_1, w_2) = \int_{-\infty}^{\infty} \int_{-\infty}^{\infty} \sum_{n_2=0}^{N_1} \sum_{n_2=0}^{N_2} Box(x_1 + n_1 T_1, x_2 + n_2 T_2) e^{iw(x_1+x_2)} dx_1 dx_2$$

$$= \int_{-\infty}^{\infty} \int_{-\infty}^{\infty} \sum_{n_2=0}^{N_1} \sum_{n_2=0}^{N_2} Box(y_1, y_2) e^{iw((y_1-n_1 T_1)+(y_2+n_2 T_2))} dx_1 dx_2$$

$$= \sum_{n_2=0}^{N_1} \sum_{n_2=0}^{N_2} \int_{-\infty}^{\infty} \int_{-\infty}^{\infty} Box(y_1, y_2) e^{iw(y_1+y_2)} e^{-iw(n_1 T_1+n_2 T_2)} dy_1 dy_2$$

$$= \sum_{n_2=0}^{N_1} \sum_{n_2=0}^{N_2} e^{-iw(n_1 T_1+n_2 T_2)} \int_{-\infty}^{\infty} \int_{-\infty}^{\infty} Box(y_1, y_2) e^{iw(y_1+y_2)} dy_1 dy_2$$

$$= \left(\sum_{n_2=0}^{N_1} \sum_{n_2=0}^{N_2} e^{-iw(n_1 T_1+n_2 T_2)} \right) \mathcal{F}^{-1}\{Box\}(w_1, w_2)$$

$$= \left(\sum_{n_2=0}^{N_1} e^{-iwn_1 T_1} \right) \left(\sum_{n_2=0}^{N_2} e^{-iwn_2 T_2} \right) \mathcal{F}^{-1}\{Box\}(w_1, w_2)$$

$$= (p_1 + iq_1)(p_2 + iq_2)\mathcal{F}^{-1}\{Box\}(w_1, w_2)$$

$$= ((p_1 p_2 - q_1 q_2) + i(p_1 p_2 + q_1 q_2))\mathcal{F}^{-1}\{Box\}(w_1, w_2)$$

$$= (p + iq)\mathcal{F}^{-1}\{Box\}(w_1, w_2)$$

Where we define $p := (p_1 p_2 - q_1 q_2)$ and $q := (p_1 p_2 + q_1 q_2)$. For this identity we used green's integration rule which allowed us to split the double

29

integral to the product of two single integrations. Also, we used the definition of the 2-dimensional inverse Fourer transform of the Box-function. We applied the same substituation like we did in for the 1 dimensional case, but this time twice, once for each variable seperately. The last step, substituting with p and q will be useful later in the implementation. The insight should be, that the product of two complex numbers is again a complex number. We will have to compute the absolute value of $\mathcal{F}^{-1}\{f\}(w_1, w_2)$ which will then be equal $(p^2 + q^2)^{\frac{1}{2}} \left| \mathcal{F}^{-1}\{Box\}(w_1, w_2) \right|$

2.3.6 Final Expression

As the last step of our series of derivations, we plug all our findings together to one big equation in order to compute the color for each pixel on our mesh in the $CIE_X YZ$ colorspace:

For a given heigh-field $h(x, y)$, representing a small patch of the nano-structure of our surface, the resulting CIE_{XYZ} caused by the effect of diffraction can be computed like the following:

Let $P(u, v, \lambda) = F_{fft}^{-1}\{i^n h^n\}\left(\frac{2\pi u}{\lambda}, \frac{2\pi v}{\lambda}\right)$

$$
\begin{pmatrix} X \\ X \\ Z \end{pmatrix} = C(\omega_i, \omega_r) \int_\lambda \sum_{n=0}^{N} \frac{(wk)^n}{n!} \sum_{(r,s) \in \mathcal{N}_1(u,v)} |P_\lambda(u - w_r, v - w_s)|^2
$$
$$
\phi(u - w_r, v - w_s) \begin{pmatrix} S_x(\lambda) \\ S_y(\lambda) \\ S_z(\lambda) \end{pmatrix} d\lambda
$$

(38)

where $\phi(x, y) = \pi e^{-\frac{x^2 + y^2}{2\sigma_f^2}}$ is the gaussian window. where w_s and w_r are ... explain them

3 Implementation

In computergraphics, we are interested in synthesizing 2d images from a given scene containing our 3d geometries by using so called shader programs. This process is dentonoted as rendering. The purpose of shader programs, which are executed directly on the GPU hardware device, is to compute the colorization and illumination of the objects living in our scene. All these computations happen in several stages and depend on the provided scene-input paramteters like the camera, light sources, objects material constants and the desired rendering effect one is interested in to model. The shader stages are implemented sequencially as small little programs, the so called vertex-, geometry- and fragment-shaders. Those stages are applied within the rendering pipeline sequencially.

Our shaders which we use are written in a highlevel language called GLSL, the OpengGL Shading Language. The decission for using OpenGL has been made since my underlying framework, which is responsible for the precomputation of all scene date, is based on another framework, written in Java using JOGL in oder to communicate with the GPU and is also responsible to precompute all the relevant scene data. This framework, the so called jrtr framework, has been developed as an exercise during the class computer graphics held by M. Zwicker which I attended in autumn 2012. The framework itself has been used and further extended during this thesis quite a lot. All necessary input data required for our java framework in order to perfrom the shading is precomputed by using Matlab. This is basically addressing all the required precomputations for the provided heigh-fields, refering to computation of the inverse two dimensional Fourier transformations which are further explained within this chapter. The matlab scripts themself rely on the provided snake nano-scaled sheds images, taken by AFM.

It's noteworthy that all the vertices are processed within the vertex-shader, whereas the fragment shader's responsibility is to perfrom pixelwise rendering, using the input from the vertex shader. Just remember, fragements are determined by a triple of vertices. hence each pixel has assigned a trilinear interpolated value of all input parameters of its spanning vertices. Usually, all necessary transformations are applied vertex-wise, considering the vertex-shader as the precomputation stage for the later rendering within the rendering pipeline, in the fragment-shader. In the geometry shader, new vertices around a considered vertex can be created. this is useful for debugging - displaying normals graphically for example.

In this part of thesis we are going to explain how we render our BRDF formulation derived in the last section in practice. all the necessary computations in order to simulate the effect of diffraction are performed within a fragment shader. This implies that we are modeling the effect of diffraction pixelwise and hence the overall modeling quality and computional pace depends on rendering window's resolution.

By the end of this chapter we will have seen how our how our render works, what we have to precompute and how our shaders work.

3.1 Precomputations in Matlab

Our first task is to precompute the inverse two dimensional discrete fourier transformations of a given snake shed patch of interest taken by AFM. For that purpose we have written a small matlab script which offers a huge collection of mathematically, nummerically fast and stable alforithmes. Our matlab script reads a given image, which is representing a nano-sclaed heightfield, and computes its inverse two dimensional DFT by using matlab's internel inverse fast fourier transformation function, denoted by $ifft2$. Note that we only require once color channel of the input image since the input image is representing an heightfield, encoded by just one color. Basically, we are interested in computing the $ifft2$ for different powers of the input image since our taylor series approximation for the overall computation relies on this. Keep in mind that taking the fourier transoformation of an arbitrary function will result in a complex valued output which imples that we will get a complex value for each pixel of our input image. Therefore, for each input image we get as many output images, representing the two dimensional inverse fourier transformation, as the minimal amount of taylor terms required for a well-enough approximation. In order to store our output images, we have to use 2 color channels instead just one like it was for the given input image. As an optimization step, we do not directly store images, rather we output binary files which contain all RGB values for each pixel in a row first, coloumn last format. This allows us to have much higher precission for the output values and also it does not waste any color channels. Note that we have scaled each pixel value in a range between 0 and 1. Therefore, we have to remember store four scaling factors for each output image as well, which are the real and imaginary minimum and maximum values. Later, using linear interpolation within the shaderm we will get back the image's original values.

Algorithm 1 Precomputation: Fourier images

```
% maxH:     A floating−point number specifying
%           the value of maximum height of the
%           height−field in MICRONS, where the
%           minimum−height is zero.
%
% dH:       A floating−point number specifying
%           the resolution (pixel−size) of the
%           'discrete' height−field in MICRONS.
%           It must less than 0.1 MICRONS to
%           ensure proper response for
%           visible−range of light spectrum.
%
% termCnt: An integer specifying the number of
%           Taylor series terms to use.

function []= ComputeFFTImages(maxH, dh, termCnt)
dH = dh*1E−6;
% load patch into patchImg
patchImg = patchImg.*maxH;
% perform imrotate(patchImg, angle)
for t = 0 : termCnt
  patchFFT = power(1j*patchImg, t);
  fftTerm{t+1} = fftshift(ifft2(patchFFT));

  imOut(:,:,1)  = real(fftTerm{t+1});
  imOut(:,:,2)  = imag(fftTerm{t+1});
  imOut(:,:,3)  = 0.5;

  % perform imrotate(imOut, −angle)
  % find real and imaginary extrema of
  % write imOut, extrema, dH, into files.
end
```

TODO: say something about output?

3.2 Our Java Renderer

In autumn 2012, during the semester I have attented the class computer
graphics held by M. Zwicker. During the whole class we have developed a
so called real time renderer program written in java as a series of homework
assignments in order to be admitted to the final exam. The architecture of
the program is divided into two parts: a rendering engine, the so called jrtr
(java real time renderer) and an application program, denoted as scene.

SHOW ARCHITECTURE GRAPHIC from CG show schema: scene da-
ta => GPU=[Vertex processing, modeling and viewing transformation =>
Projection => Rasterization, fragment processing, visibility] => image

the scene application program task was basically to define the whole sce-
ne we is going to be rendered within jrtr later. A scene consists of the setup
of the world camera, definitions of light source, frustum, geometries which
live in our scene and their material constants. Such materials are textures for
example. All those scene attributes are managed within jrtr. In the applicati-
on program, there only happens their definition. The minimal definition of a
geometry is given by its wireframe mesh. This is a datastructures consisting
of vertices each stored as a triple of xyz positions in an float array and tri-
angles each defined by a triple of vertex-indices which form a fragment each
stored in an integer array. It is possible to assing additional geoemtry data
like a color for each vertex, normals and texture coordinates. All whole scene
is stored within container data-structures, defined and managed within jrtr,
like a scene graph, which contains all geometries and their transformations in
a tree like structured hierarchy. The geometries themself are stored within an
container, containing all vertex attributes and the material constants. The
jrtr rendering engine uses a low-level API, called openGL in order to com-
municate with the grpahcis processor unit (GPU). Within jrtr, the whole
resource-management for the rendering pipeline place, i.e. all required low-
level buffers are allocated, flushed and assigned by the scene data attributes.
jrtr also offers also the possibility to assign arbitrary shaders.

3.2.1 Scene

what is done here reworked such that it is mvc-architecute based user-interaction:
handlers in gui. which geometries are defined what material constants are de-

fined: mention fabricators: light, camera, materials,... file readers: monkey

3.2.2 jrtr Framework

shader tasks assign all shader inputs: like t0 and so on load fourier images and assign to buffers snapshot functionality shaders: diffraction shader

3.3 GLSL Diffraction Shader

TODO: start using the final findings from chapter 2 and substitute

3.3.1 Vertex Shader

The first computional stage within our rendering pipeline is computing all necessary per vertex data. Those computations are preformed in the vertex shader. In our case, we compute for any vertex of our current geometry the direction vectors $k1$ and $k2$ described like previousely in the tangent space. Initially all input data lives in its own space. Hence, we first have to transfrom all input data into the same space in order to use it for later computations within the fragment shader. We are going to transform k1 and k2 into the so called tangent space which. Furthermore, we have also to realign our local coordinate system. This is why there is an rodrigues rotation also involved. In order to avoid scaling issues and since we are only interested in the direction of the vectors k1 and k2, we have to normalize them, too. Last, we also output the position of the current vertex transfomed into the projective camera space.

explain cop_w modelM other shader assigned inputs

3.3.2 Fragment Shader

The purpose of a fragment shader is to render per fragment. A fragment is spaned by three vertices of a given mesh. For each pixel within all the output from the vertex shaders of its corresponding vertices is then trilinearly interpolated, depending on the pixel's position within the fragment, and passed into its fragment shader program. Furthermore, there can be additional input be assigned which is not directly interpolated from the output of vertex shader programs. Our fragment shader just relies on k1 and k2 from its vertex shaders for the computation of the effect of diffraction. There are some values preliminarily assigned to our fragment shader during the opgengl setup

---

Algorithm 2 Vertex diffraction shader

---

foreach *Vertex v* ∈ *Shape* **do**

    *vec*3*N* = *normalize*(*modelM* ∗ *vec*4(*normal*, 0.0))*.xyz*

    *vec*3*T* = *normalize*(*modelM* ∗ *vec*4(*tangent*, 0.0))*.xyz*

    T = *rotateRodrigues*(*T*, *N*, *phi*)

    *vec*3*B* = *normalize*(*cross*(*N*, *T*))

    *vec*3*Pos* = ((*cop*$_w$ − *position*))*.xyz*

    *vec*4*lightDir* = (*directionArray*[0])

    lightDir = *normalize*(*lightDir*)

    l = *projectVectorOnTo*(*lightDir*, *TangentSpace*)

    p = *projectVectorOnTo*(*Pos*, *TangentSpace*)

    normalize(*l*); *normalize*(*p*)

    gl$_P$*osition* = *projection* ∗ *modelview* ∗ *position*

end for

---

within our java program, like all references to the image buffers, containing the fourier transformations, the number of taylor step approximations, the minimal and maximal wavelength, other lookup values like the scaling factors, a reference to a lookup table containung the cie xyz color weights for our wavelength domain and other scaling constants.

Our shader performs an on-thefly numerical integration for the integral in the derivation using trapeziodal rulewith uniform discretization of the λ dimsension at a resolution of 5nm. To compute $F_{dtft}\{p\}$ terms the shader uses he precomputed DFTs for the Taylor series terms given in the derivation. The Gaussian winow approach is perfromed for each discrete λ value using a window large enough to span $4\sigma_f$ in both dimensions. For computing DFT tables we generally use nanostructure gieghtfields that span at least $65\mu m^2$ and are sampled with resoution of at least 100nm. This ensures that the spectral response encompasses al the wavelengths in the visible spectrum, i.e. from 380nm to 780nm. Note that this shader is not very fast in hardly can be denoted being interactive.

mention we uniform discretize λ for a given (u,v) which implies compressing sampled frequencies to the region near to the origin (of their frequency domain). For natural structures in nano-scale, most of their spectral energy lies at lower spatial frequencies which maps closer to region $(u, v) = (0, 0)$ than higher frequencies. This is why We have chosen to sample (u,v) space non-linearly. We use 30 taylorterms for our approximation approach which

has an error below Y, proven in the previous derivation chapter.

From line 4 to 26:
Within this loop happens the uniform sampling along lambda space. At line 5: $getClrMatchingFnWeights(\lambda)$ computes the color weights for the current wavelength by bilinear interpolation from the two closest given CIE_{XYZ} color weights for our current wavelength λ. At line 6: $getLookupCoord(u, v, \lambda)$ computes the current coordinate for the texture lookup in our precomputed ifft2 images.

From line 9 to 24:
Within this loop happens the taylor series approximation till a predefined upper bound, denoted as $MAXTAYLORTERMS$. Basically, the spectral response is approximated for our current (u, v, λ). Furthermore, neighborhood-bounds for the upcoming gaussian windowing-sampling-approach are computed, denoted as anchorX and anchorY.

From line 14 to 22:
In this most inner loop the convolution of the gaussian window with the inverse fft of the patch is pixelwise performed. $getGaussWeightAtDistance(dist)$ computes (29) from the distance between the center of the fft image with the current position in the neighborhood in texture space. $getRescaledFourierTextureValueAt(positi$ rescales the current computed value by the precomputed extrema values since all image values are scaled between 0 and 1. At line 27 $C(\hat{\mathbf{k}_1}, \hat{\mathbf{k}_2})$ is multiplied in front of the current computed pixelColor. This terms was introduced in the derivation chapter and is the product of equation (21)

The C term includes the so called Fresenel Term. We compute this by using the so called Schlick approximation (See appendix) using an reactive index at 1.5 since this is close to the measured value from snake sheds. NOTE about shadow function: Our BRDF values are scaled by s shadowing function as described in (SEE REFERENCES - PAPER), since most of the grooves in the snake skin nanostructures would from a V-cavity along the plane for a wave front with their top-edges at almost the same height.

SHOW GRAPH for this fact: (lambda, k=f(lambda)), where $k = \frac{2pi}{\lambda}$, $f = \frac{c}{\lambda}$

Algorithm 3 Fragment diffraction shader

1: **foreach** *Pixel $p \in$ Fragment* **do**
2:     **INIT** $BRDF_{XYZ}, BRDF_{RGB}$ **TO** $vec4(0.0)$
3:     $(u, v, w) = \hat{\mathbf{k_1}} - \hat{\mathbf{k_2}}$
4:     **for** $(\lambda = \lambda_{min};\ \lambda \leq \lambda_{max};\ \lambda = \lambda + \lambda_{step})$ **do**
5:         $xyzWeights = getClrMatchingFnWeights(\lambda)$
6:         $lookupCoord = getLookupCoord(u, v, \lambda)$
7:         **INIT** P **TO** $vec2(0.0)$
8:         $k = \frac{2\pi}{\lambda}$
9:         **for** $(n = 0$ **TO** $MAXTAYLORTERMS)$ **do**
10:             $taylorScaleF = \frac{(kw)^n}{n!}$
11:             **INIT** F_{fft} **TO** $vec2(0.0)$
12:             $anchorX = int(floor(center.x + lookupCoord.x * fftImWidth)$
13:             $anchorY = int(floor(center.y + lookupCoord.y * fftImHeight)$
14:             **for** $(i = (anchorX - winW)$ **TO** $(anchorX + winW + 1))$ **do**
15:                 **for** $(j = (anchorY - winW)$ **TO** $(anchorY + winW + 1))$ **do**
16:                     $dist = getDistVecFromOriginFor(i, j)$
17:                     $position = getLocalLookUp(i, j, n)$
18:                     $fftVal = getRescaledFourierTextureValueAt(position)$
19:                     $fftVal *= getGaussWeightAtDistance(dist)$
20:                     $F_{fft} += fftVal$
21:                 **end for**
22:             **end for**
23:             $P += taylorScaleF * F_{fft}$
24:         **end for**
25:         $xyzPixelColor += dot(vec3(|P|^2), xyzWeights)$
26:     **end for**
27:     $BRDF_{XYZ} = xyzPixelColor * C(\hat{\mathbf{k_1}}, \hat{\mathbf{k_2}}) * shadowF$
28:     $BRDF_{RGB}.xyz = D_{65} * M_{XYZ-RGB} * BRDF_{XYZ}.xyz$
29:     $BRDF_{RGB} = gammaCorrect(BRDF_{RGB})$
30: **end for**

3.4   Discussion

Optimization: Just use a few lambdas (just those which are at least required), which will enhance the overall runtime quite a lot but the overall accuracy will suffer then, too.

one which basically samples the whole lambda space using a gaussian window. This shader will be modeling the effect of diffraction completely but will also be rather slow. The other shader will use a gaussian window too but will just use a few wavenumber for the sampling process. Furthermore, this shader will thread specularity seperatly as a special case which will be more like an approximation.

how from $cie_x yz$ to $cie_r gb$ how gamma correction how texturing

4 Evaluation Data Acquisition

what is this chapter about how is evaluation perfromed our shader evaluation java table generator provided by daljit. explain how this program works: subvariants: sample whole lambda space, just a few lambdas, pq approach. how from those generated tables to matlab how to read those discussion

The true surface topography is extracted by flattening a single snake scale on a metal disc covered with carbon adhesive tape. Then, measurements were carried out using intermittment contact mode in a Bruker Dimension 3100 atomic force microscope (AFM) under ambient conditions, using a nanoscope V controller. The tops used were etched silicon TESP tips with a nomminal frequency and force constant of 320 kHz and 42 N/m respectively.

In order to check the physical reliability of our mthod we used our method as a virtual diffraction experimental bench on a syntetic blazed grating, Elaphe and Xenopeltis snakes. When light at a wavelength λ falls on a sample presenting a periodicity a along the incident plane under an incident angle θ compared to the normal of the surface the angle ϕ corresponding to the direction of the emerging beam showing constructive interferences (maximum in intensity) is given by

GRATING EQUATION

where m is the order of diffraction.

SHOW PLOTS AND TALK ABOUT THEM

4.1 Diffraction Gratings

Gratings may be of the reflective or transmissive type, analogous to a mirror or lens respectively. A grating has a zero-order mode (where m=0), in which there is no diffraction and a ray of light behaves according to the laws of reflection and refraction the same as with a mirror or lens respectively.

An idealised grating is considered here which is made up of a set of slits of spacing d, that must be wider than the wavelength of interest to cause diffraction. Assuming a plane wave of wavelength   with normal incidence (perpendicular to the grating), each slit in the grating acts as a quasi point-source from which light propagates in all directions (although this is typically limited to a hemisphere). After light interacts with the grating, the diffracted light is composed of the sum of interfering wave components emanating from each slit in the grating. At any given point in space through which diffracted light may pass, the path length to each slit in the grating will vary. Since the

path length varies, generally, so will the phases of the waves at that point from each of the slits, and thus will add or subtract from one another to create peaks and valleys, through the phenomenon of additive and destructive interference. When the path difference between the light from adjacent slits is equal to half the wavelength, /2, the waves will all be out of phase, and thus will cancel each other to create points of minimum intensity. Similarly, when the path difference is , the phases will add together and maxima will occur. The maxima occur at angles m, which satisfy the relationship dsin m/ =|m| where m is the angle between the diffracted ray and the grating's normal vector, and d is the distance from the center of one slit to the center of the adjacent slit, and m is an integer representing the propagation-mode of interest.

Thus, when light is normally incident on the grating, the diffracted light will have maxima at angles θ_m given by:

$$dsin(\theta_m) = m\lambda$$

It is straightforward to show that if a plane wave is incident at any arbitrary angle i, the grating equation becomes:

$$d(sin(\theta_i) + sin(\theta_m)) = m\lambda$$

When solved for the diffracted angle maxima, the equation is:

$$sin(\theta_m) = \left(\frac{m\lambda}{d} - sin(\theta_i)\right)$$

The light that corresponds to direct transmission (or specular reflection in the case of a reflection grating) is called the zero order, and is denoted m = 0. The other maxima occur at angles which are represented by non-zero integers m. Note that m can be positive or negative, resulting in diffracted orders on both sides of the zero order beam.

This derivation of the grating equation is based on an idealised grating. However, the relationship between the angles of the diffracted beams, the grating spacing and the wavelength of the light apply to any regular structure of the same spacing, because the phase relationship between light scattered from adjacent elements of the grating remains the same. The detailed distribution of the diffracted light depends on the detailed structure of the grating elements as well as on the number of elements in the grating, but it will always give maxima in the directions given by the grating equation.

$$\forall \begin{pmatrix} x \\ y \\ z \end{pmatrix} \in \mathbb{R}^3 : \exists r \in [0, \infty) \exists \phi \in [0, 2\pi] \exists \theta \in [0, \pi] \text{ s.t.}$$

$$\begin{pmatrix} x \\ y \\ z \end{pmatrix} = \begin{pmatrix} rsin(\theta)cos(\phi) \\ rsin(\theta)sin(\phi) \\ rcos(\theta) \end{pmatrix}$$

4.2   Matlab code

4.3   Discussion

5 Results

show all views results. differece of this shader compared to evaluation shader show real snake images for comparison with real rendered images show experiments received show rendered images by daljits implemetation of stams approach. show our renderer's results mention all input parameters and their values. mention system specs and how long it took in order to precompute show some idft2 images, used patch, besids rendered image what initial size was used patch? mention GEM results. mention real results from geneva - use same paramter setup.

6 Conclusion

can we do better?

brief overwiew pf results achieved, what was the most important in the work, appropriate to provide an introduction to possible future work in this field. reflect the emotions associated with the work, what was especially difficult or particularly interesting, one may elaborate on open questions within subjects related to the thesis without giving any answer. discuss follow-ups.

statment what you've researched and what your original contribution of the fild is explain why our approach is a good idea explain how the straight foreward approach would behave compared to our approach, computing the fourier transformations straight away. explain what we achieved, summary say something about draw-backs and about limitations of current apporach say something about the ongoing paper future work maybe say something about runtime complexity

6.1 Further Work

6.1.1 References

- [**1**] http://en.wikipedia.org/wiki/Ratio_test

- [**2**] http://math.jasonbhill.com/courses/fall-2010-math-2300-005/lectures/taylor-polynomial-error-bounds

7 Acknowledgment

ty to abcdefg

8 TODOs

when use aplitude approach? finish-up previous work.